Food Biophysics (2026) 21:68
https://doi.org/10.1007/s11483-026-10160-6

RESEARCH

Novel Hazelnut Protein Isolate-Polysaccharide Conjugates for Microencapsulation of *Lactobacillus Acidophilus*: Effects on Microstructure, Digestion Resistance, and Storage Stability

Ilyas Atalar[1] · Hatice Elen[1,2] · Abdullah Kurt[3] · Nevzat Konar[4]

Received: 18 January 2026 / Accepted: 15 May 2026
© The Author(s) 2026

Abstract

This study investigated the potential of hazelnut protein isolate (HPI) in conjugation with sodium alginate (SA) or gum arabic (GA) as novel wall materials for the microencapsulation of *Lactobacillus acidophilus* via spray drying. The effects of different inlet air temperatures (130 °C and 160 °C) and pump rates (10 and 15 mL/min) on the survival, morphological characteristics, and storage stability of the probiotics were evaluated. All microencapsulated formulations maintained high viability (>7.0 log CFU/g) after drying, successfully exceeding the therapeutic threshold. SEM observations showed that GA-HPI matrices formed smoother and more spherical microcapsules, and SA-HPI matrices exhibited a more rugose and compact structure. Encapsulation significantly improved the resistance of *L. acidophilus* against simulated gastric fluid (pH 3.0), with GA-HPI-1 exhibiting the highest gastric survival ratio (66.07%). Conversely, SA-HPI formulations, particularly SA-HPI-3 (160 °C, 10 mL/min), showed superior performance during a 60-day storage period. The enhanced stability of the SA-HP-3 formulation is hypothesized to be linked to the potential formation of a dense, glassy matrix, as suggested by the high outlet temperature (82 °C) and the resulting low water activity. At an aw of 0.185, molecular mobility is expected to be significantly restricted, which likely contributed to the immobilization of the probiotic cells and the prevention of metabolic degradation. Kinetic modeling using linear regression showed that the GA-HPI conjugates maintained viability well for the first 15 days, but a breakdown occurred after the 30th day. These findings demonstrate that hazelnut protein-polysaccharide conjugates are effective plant-based carriers for probiotics, with the SA-HPI system offering exceptional long-term stability for functional food applications.

Keywords protein polysaccharide conjugates · hazelnut protein isolate · microencapsulation · spray drying · storage stability · gastrointestinal survival

Introduction

Probiotics are defined as live microorganisms that, when administered in adequate amounts, confer a health benefit on the host [1, 2]. These benefits include modulation of the intestinal microbiota, stimulation of the immune system, and prevention of gastrointestinal disorders [3]. However, to provide these therapeutic effects, probiotic bacteria must survive in the food product during storage and resist passage through the gastrointestinal tract, arriving in the colon with a minimum viability typically recommended at 10^6-10^7 CFU/g. The sensitivity of probiotics to environmental stresses such as heat, oxygen, and gastric acidity poses a significant challenge to their effective application in functional foods [4].

✉ Ilyas Atalar
ilyas.atalar@ogu.edu.tr

1 Agriculture Faculty, Food Engineering Department, Eskisehir Osmangazi University, Eskisehir, Turkey

2 Tayas Food R&D Centre, Gebze, Kocaeli, Turkey

3 Chemical and Metallurgical Engineering Faculty, Food Engineering Department, Yildiz Technical University, Istanbul, Turkey

4 Agriculture Faculty, Dairy Technology Department, Ankara University, Ankara, Turkey

Published online: 22 May 2026

Microencapsulation has emerged as a widely adopted technology to enhance the stability and viability of probiotics by entrapping them within a protective matrix [5]. Among encapsulation techniques, spray drying is the most commonly used method in the food industry due to its low cost, high production efficiency, and continuous processing capabilities [6]. Nevertheless, the high temperatures inherent to the spray drying process can induce thermal and dehydration stress, leading to cell membrane damage and reduced viability [7]. Therefore, selecting appropriate wall materials is critical to provide a physical shield and to stabilize cellular components during drying and subsequent storage [8]. Traditionally, animal-derived proteins such as whey protein and casein have been utilized as encapsulating agents due to their excellent film-forming and emulsifying properties [9]. However, rising consumer demand for plant-based alternatives, driven by concerns about sustainability and dietary restrictions, has shifted the focus toward plant proteins [10]. While plant proteins offer a sustainable alternative, they may sometimes exhibit limitations in solubility or emulsification compared to animal proteins and to overcome these limitations and enhance encapsulation efficiency, proteins are often modified [11, 12]. To meet sustainable development goals, the energy and cost efficiency of conventional physical and biological methods for plant-based protein modifications must be reconsidered. Maillard reactions provide a chemical reagent-free pathway to obtain novel protein-sugar conjugates. This aligns with the clean-label trend and positions the Maillard reaction as a key modification strategy for plant-based proteins within the framework of food safety regulations [13]. The conjugation of proteins with polysaccharides, often achievable through the Maillard reaction or electrostatic complexation, can form a denser network structure that improves the barrier properties against environmental stressors [4]. The fundamental advantages of these biopolymer conjugates are multifaceted. Conjugation provides enhanced emulsification and structural integrity. While proteins are excellent amphiphilic emulsifiers, they are often susceptible to environmental stressors, such as pH and ionic strength [14]. Conjugation with polysaccharides creates a robust viscoelastic layer around oil droplets, offering steric hindrance that prevents coalescence [15]. Furthermore, polysaccharides act as fillers, occupying pores and cracks in the protein matrix, resulting in a compact, smooth surface that physically shields probiotics from oxygen and moisture.

Conjugates offer superior protection during thermal processing, such as spray drying. According to the water replacement theory, the sugar moieties in the conjugates stabilize the cell membrane by forming hydrogen bonds with phospholipid head groups, thereby preventing phase transitions and dehydration damage [16]. Additionally, Maillard reaction products (MRPs) enhance the thermal stability of the wall material, significantly increasing cell viability during pasteurization [17]. The hybrid structure ensures gastrointestinal resistance and controlled release of the active ingredient. The high buffering capacity of proteins, combined with the dense network of polysaccharides, slows the diffusion of gastric acids. These conjugates exhibit resistance to pepsin hydrolysis due to steric hindrance, preventing premature release in the stomach. Subsequently, their pH-responsive nature enables targeted delivery, as the capsules swell or degrade in the neutral/alkaline environment of the intestines [18].

Sodium alginate, a natural anionic polysaccharide, is frequently used for its pH-responsive release properties [19], while gum arabic is renowned for its emulsification capacity and stability [20]. Although extensive research exists on the microencapsulation of probiotics using legume proteins, such as soy protein [21, 22], mung bean protein [23], and peanut [24]. There is limited information regarding the potential of hazelnut protein conjugates as wall materials. Studies on the encapsulation and delivery of functional factors in gel systems prepared from Maillard reaction products of various plant proteins and polysaccharides remain underexplored [25]. This study aims to bridge this gap by developing hazelnut protein-gum arabic and hazelnut protein-sodium alginate conjugates to encapsulate *Lactobacillus acidophilus* via spray drying. The specific objectives were to investigate the effects of different inlet air temperatures and pump speeds on the physicochemical properties and morphology of microcapsules, and to evaluate the viability of the encapsulated bacteria during spray drying, storage, and in vitro gastrointestinal digestion.

Materials and Methods

Materials

For this study, blanched Turkish Tombul hazelnuts (Corylus avellana) were sourced from Yavuzkan Hazel Gıda (Giresun, Türkiye). The oil was extracted using a pilot-scale cold press (Ugurluoglu, Konya, Türkiye), yielding a hazelnut meal with 97.33% dry matter, 24.66% protein, 2.85% ash, and 45.25% oil. This meal served as the base for isolating hazelnut protein. Sodium alginate (SA) was obtained from Sigma-Aldrich (St. Louis, USA).

Methods

Protein Isolation

Hazelnut protein was extracted using the protocol described by Sarıcaoğlu et al. [26]. First, the hazelnut meal pellets were ground into a fine powder. This powder was mixed

with purified water at a 1:12 (w/v) ratio and homogenized for 3 min at 9,000 rpm (Ultra-Turrax, IKA T18, Germany). To solubilize the proteins, the pH was adjusted to 12.0 using 5 M NaOH while stirring. The suspension was then centrifuged (9,000 rpm, 15 min, 4 °C) to separate the soluble fraction. This extraction was repeated three times. We then precipitated the proteins at their isoelectric point (pH 4.5), collected the resulting slurry, and lyophilized it at −55 °C for four days (Teknosem, Toros TRS-4/4V, Türkiye) to produce the final hazelnut protein isolate (HPI) powder. The composition of the HPI was verified using AOAC (2000) standards. The resulting isolate contained 97.05% dry matter, 80.15% protein, 10.15% fat, 5.85% carbohydrate (calculated by difference), and 1.60% ash [10].

Wet Heating Conjugation

Wet heating conjugation process conditions were determined in our previous studies for optimum SA-HPI conjugates (65 °C, 5 h, and 35% hazelnut protein content) [10] and for optimum GA–HPI conjugates (70 °C, 6 h, and 45% hazelnut protein content) [27]. These conditions were determined according to the maximum glycation degree, solubility, emulsion activity, and minimum HMF concentration in previous studies. The proteins and saccharides were dissolved in a phosphate buffer (pH 7.0) and stirred overnight at 300 rpm to ensure full hydration at 6% concentration.

Bacterial Enrichment and Enumeration

The enrichment protocol, described by Amiri et al. [28] was used to prepare probiotic cultures. Initially, 0.5 g of *Lactobacillus acidophilus* was inoculated into 5 mL of MRS broth and incubated aerobically at 37 °C for 24 h. To scale up biomass production, these cultures were transferred to 95 mL of MRS broth and incubated for an additional 24 h under the same conditions. To harvest the biomass, the cultures were centrifuged at 4,000 × g for 10 min at 4 °C. After discarding the supernatant, the cell pellets were washed twice with sterile, unbuffered isotonic NaCl solution to remove residual media. The final pellets were resuspended in the same saline solution to achieve a standardized bacterial suspension of 9–10 log CFU/mL for the microencapsulation process. Despite minor variations in the initial counts between experimental batches (8.75–9.41 log CFU/mL), all subsequent performance indicators, including encapsulation efficiency (%) and survival ratios (%), were calculated relative to the specific initial load (N_0) of each sample to ensure objective comparability between the SA-HPI and GA-HPI systems. For bacterial enumeration, we used the pour-plate method with MRS agar. Free *L. acidophilus* samples were serially diluted in peptone water, plated, and incubated at 37 °C for 72 h. All counts were recorded as colony-forming units (log CFU/mL).

Microencapsulation Process

Spray drying was used to microencapsulate *L. acidophilus*. An emulsion was prepared by combining a 10% (v/v) conjugate solution with a saline (FTS) solution containing the bacteria at a concentration of 10^9 CFU/mL. Throughout the process, a constant feed rate and coating-to-cell ratio were maintained. Based on preliminary trials, two inlet temperatures (130 °C and 160 °C) and two pump rates (10 mL/min and 15 mL/min) were tested to optimize the encapsulation process. As the solubility of hazelnut protein is low (15.23%), only hazelnut protein isolate couldn't be used as a control due to nozzle clogging.

Bacterial Enumeration and Encapsulation Efficiency

To calculate encapsulation efficiency (EE), the method of Semyenov et al. [29] was followed. A 0.1-g sample of the spray-dried capsules was dissolved in 9.9 mL of phosphate buffer using a magnetic stirrer for 10 min. Serial dilutions were prepared in 0.1% peptone water, and viable cell counts were determined using the pour-plate method on MRS agar. Efficiency was calculated using the following equation (Eq. 1).

$$Encapsulation\ efficiency\ (\%) = 100\mathrm{X}\ \frac{\mathrm{N}}{\mathrm{N_0}} \quad (1)$$

where N_0 represents the viable count before drying (CFU/g) and N represents the count after drying (CFU/g).

In Vitro Digestion Simulation

To evaluate the survival of encapsulated *L. acidophilus* under gastrointestinal stress, we employed the standardized static in vitro digestion protocol developed by Brodkorb et al. [30]. This procedure sequentially simulates the oral, gastric, and intestinal phases. For the oral phase, 0.1 g of encapsulated probiotics was combined with 3.5 mL of simulated salivary fluid (SSF), 0.5 mL of α-amylase solution, 25 µL of $CaCl_2$, and 975 µL of distilled water. The mixture was adjusted to pH 7.0 using 1 M NaOH and incubated at 37 °C for 2 min. To simulate gastric conditions, the oral bolus was mixed with 6 mL of simulated gastric fluid (SGF), 1.28 mL of pepsin solution, 556 µL of distilled water, and 4 µL of $CaCl_2$. The pH

was adjusted to 3.0 using 1 M HCl, and the suspension was incubated at 37 °C for 2 h. At the end of this phase, a 1 mL aliquot was collected to determine bacterial viability using the pour plate method. The remaining gastric chyme was mixed with 7.7 mL of simulated intestinal fluid (SIF), 3.5 mL of pancreatin, 1.75 mL of bile salts, 917 µL of distilled water, and 28 µL of $CaCl_2$. After adjusting the pH to 7.0 with 1 M NaOH, the mixture was incubated at 37 °C for a final 2 h. Survival rates following the intestinal phase were then determined by analyzing a 1 mL sample via the pour-plate technique on MRS agar. The gastric and intestinal survival of probiotics was assessed with the following equations (Eq. 2, Eq. 3).

$$Gastric\ Survival\ Ratio\ (\%) = 100\mathrm{x}\frac{\mathrm{Ng}}{\mathrm{N_0}} \quad (2)$$

where N_0 represents the viable count after drying (CFU/g) and N_g represents the count after gastric digestion (CFU/g).

$$Intestinal\ Survival\ Ratio\ (\%) = 100\mathrm{x}\frac{\mathrm{Ni}}{\mathrm{N_0}} \quad (3)$$

where N_0 represents the viable count after drying (CFU/g) and N_i represents the count after intestinal digestion (CFU/g).

Water Activity

Water activity (aw) values were determined using a water activity analyzer (Water Lab, Steroglass, Umbria, Italy).

SEM Imaging

The surface morphology of the microcapsules was characterized using Scanning Electron Microscopy (JSM-7001 F Jeol, Japan). To ensure high-resolution imaging and prevent charging, the microcapsules were sputter-coated with a 10 nm layer of gold-palladium using a Quorum SC7620 coater (UK). Micrographs were captured at 500×, 1000×, and 2000× to provide detailed views of structural morphology.

Storage Stability and Inactivation Kinetics

To evaluate shelf-life, capsules were stored in high-density polyethylene bottles at 4 °C for 60 days. Viable counts were performed on days 0, 15, 30, and 60 by dissolving the capsules in phosphate buffer and incubating them on MRS agar at 30 °C for 72 h. The degradation of the bacteria was modeled using first-order reaction kinetics (Eq. 4).

$$In\,(N) = -kt + In\ (N_0) \quad (4)$$

In this model, N is the cell count at time t (days), N_0 is the initial count, and k is the inactivation rate constant [31]. The linear kinetic models for GA-HPI (Fig. 1), SA-HPI (Fig. 2), GA (Fig. 3), and SA (Fig. 4) are presented.

The survival of probiotics after 60-day storage were assessed with the following equations (Eq. 5).

$$Storage\ Survival\ Ratio\ (\%) = 100x\frac{Ns}{N_0} \quad (5)$$

where N_0 represents the viable count after drying (CFU/g) and N_s represents the count after 60-day storage (CFU/g).

Statistical Analysis

To ensure high data reliability and minimize experimental error, all microencapsulation processes were conducted in duplicate, with each resulting sample analyzed in triplicate ($n = 2 \times 3$). SPSS 23.0 (IBM Corp., Armonk, NY, USA) was used for statistical analysis. Significant differences between the samples were determined through one-way Analysis of Variance (ANOVA), followed by Tukey's post-hoc test for multiple comparisons. Results were considered statistically significant at a confidence level of $p < 0.05$.

Results and Discussion

Bacterial Enumeration and Encapsulation Efficiency

The survival of *L. acidophilus* after the spray drying process and the subsequent encapsulation efficiency (EE) of the hazelnut protein isolate (HPI) based formulations are presented in Table 1. The initial bacterial count in the feed suspension was approximately 8.75–9.41 log CFU/mL. Following the spray drying process, the viable cell counts in the microcapsules ranged from 7.12 to 7.86 log CFU/g (for HPI-SA) and 7.61–8.06 log CFU/g (for HPI-GA). Despite the high thermal stress associated with spray drying, all formulations maintained a viability level above the therapeutic threshold of 10^6-10^7 CFU/g, which is required for a product to be considered a functional probiotic food [2]. One of the selection criteria for conjugation of wall materials (depending on conjugation temperature, time and protein: polysaccharide ratio) was the maximum grafting degree. The covalent bonds between proteins and polysaccharides, to a certain extent, increase the degree of grafting (DG). This contributes to the formation of a denser and more durable barrier around probiotics.

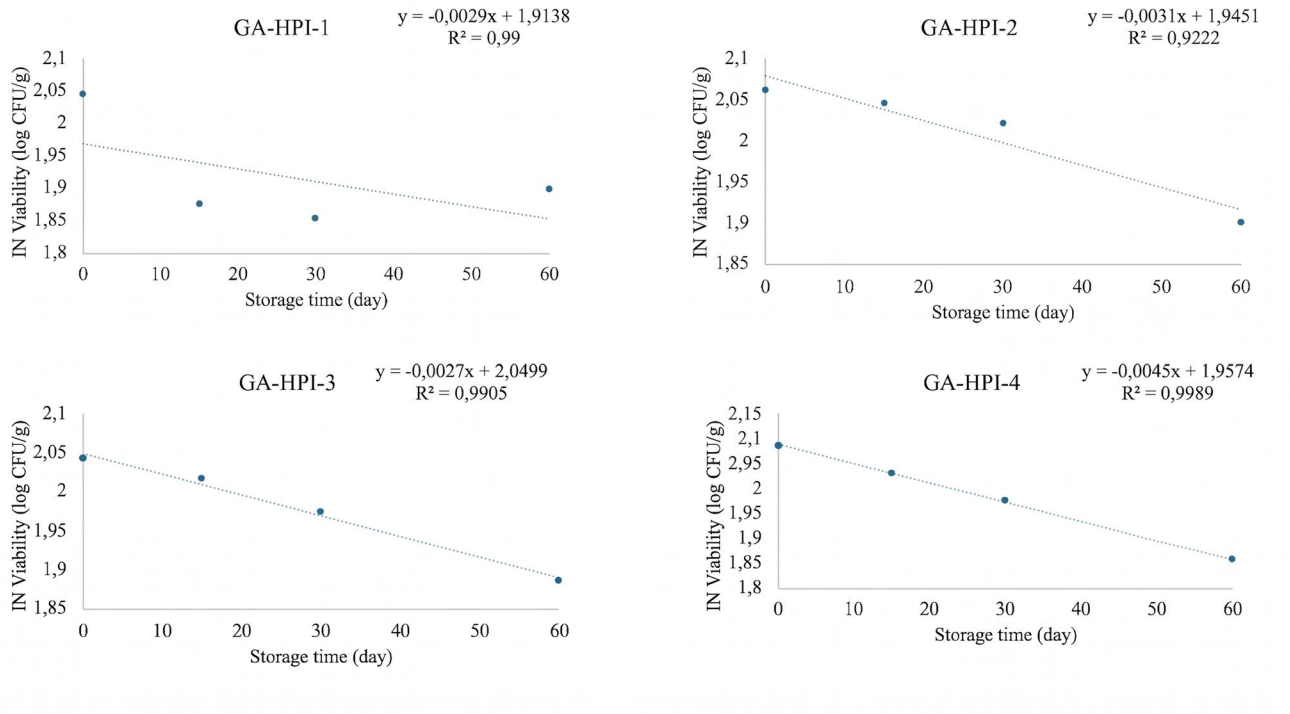


Fig. 1 Viability of *L. acidophilus* encapsulated in GA-HPI conjugates during 60 days of storage at 4 °C. (GA-HPI−1: 130 °C, 10 mL/min; GA-HPI−2: 130 °C, 15 mL/min; GA-HPI−3: 160 °C, 10 mL/min; GA-HPI−4: 160 °C, 15 mL/min)

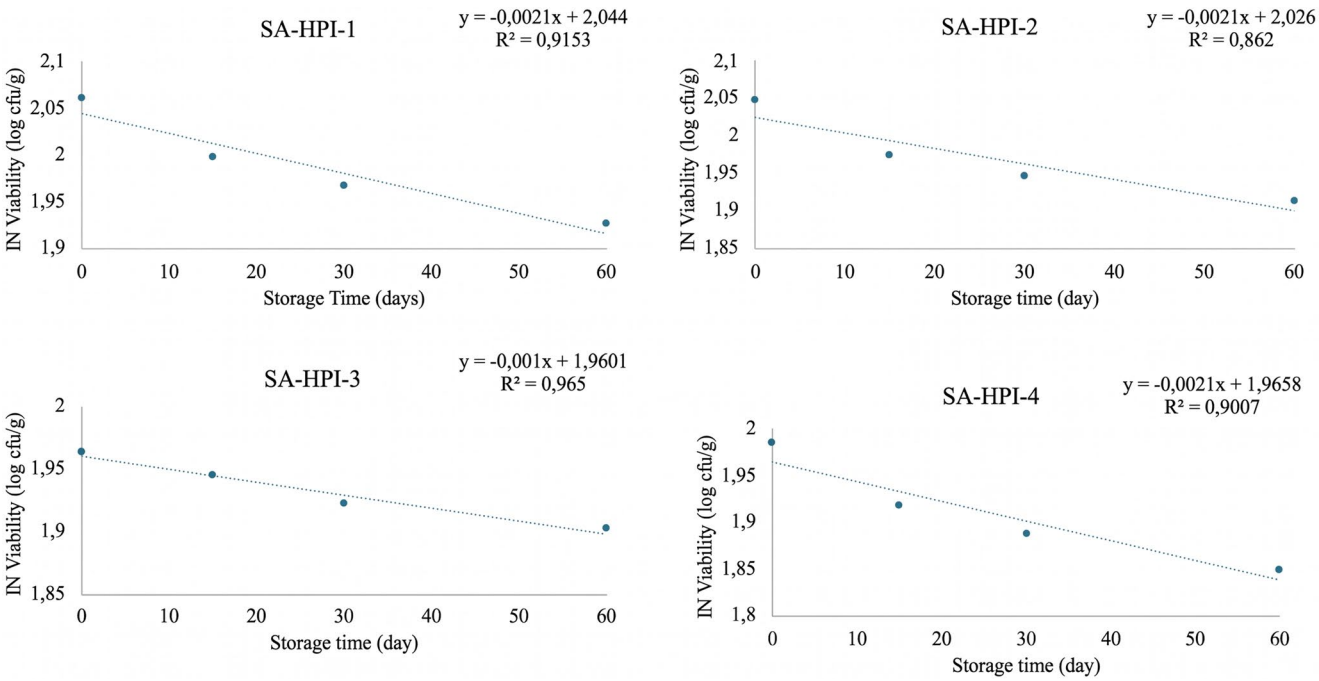


Fig. 2 Viability of *L. acidophilus* encapsulated in SA-HPI conjugates during 60 days of storage at 4 °C. (SA-HPI−1: 130 °C, 10 mL/min; SA-HPI−2: 130 °C, 15 mL/min; SA-HPI−3: 160 °C, 10 mL/min; SA-HPI−4: 160 °C, 15 mL/min)

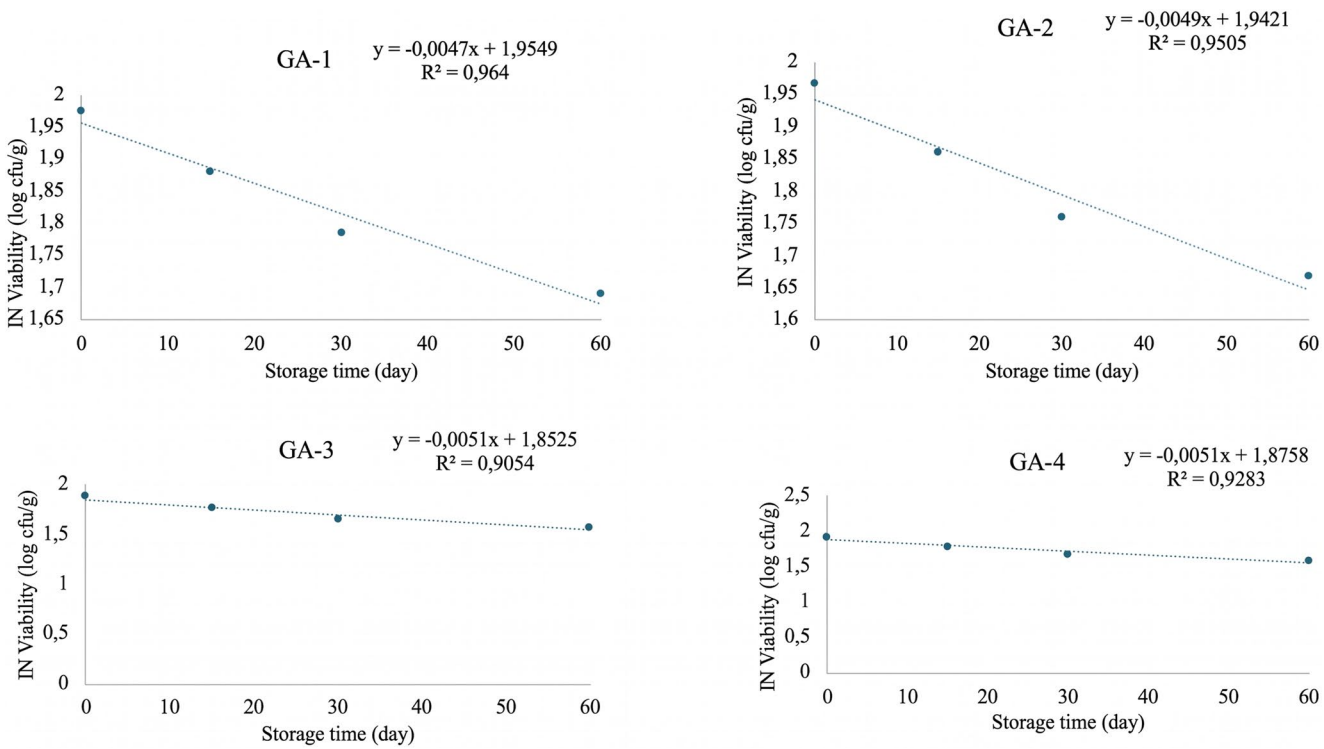


Fig. 3 Viability of *L. acidophilus* encapsulated in GA wall material during 60 days of storage at 4 °C. (GA-1: 130 °C, 10 mL/min; GA-2: 130 °C, 15 mL/min; GA-3: 160 °C, 10 mL/min; GA-4: 160 °C, 15 mL/min)

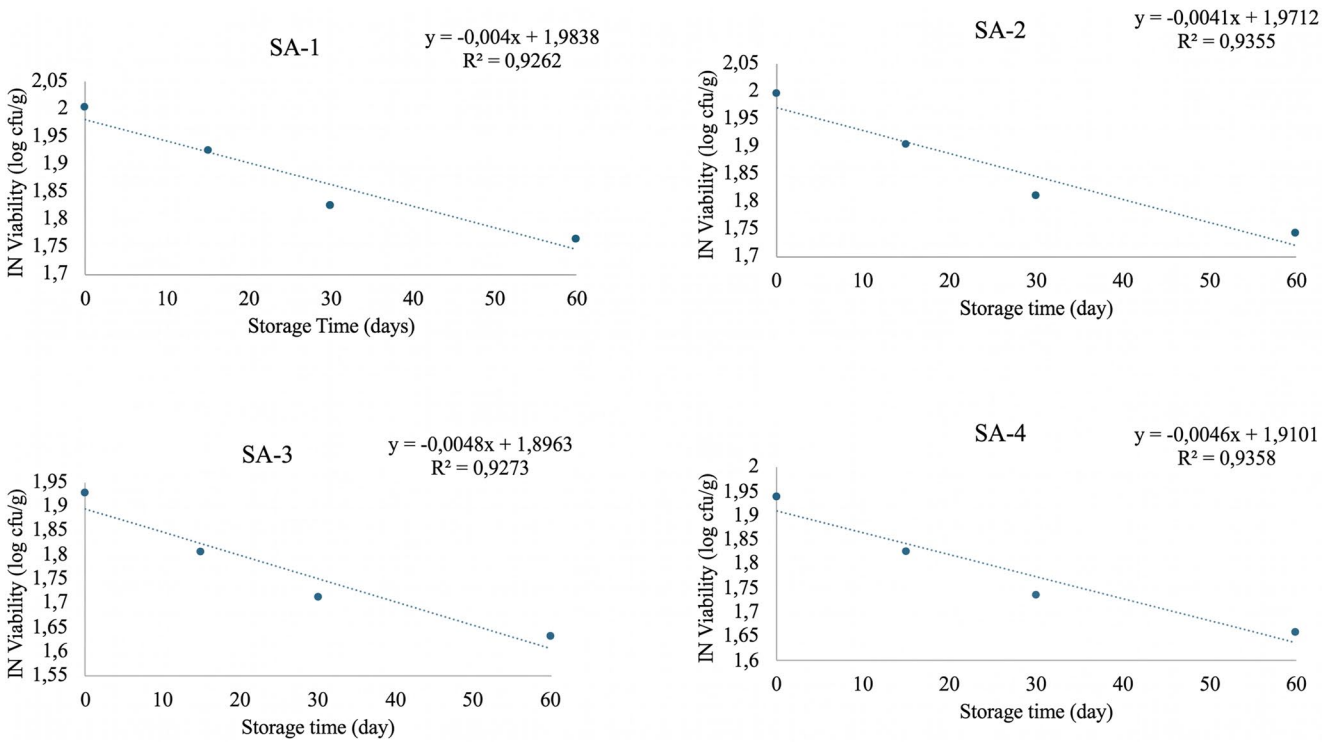


Fig. 4 Viability of *L. acidophilus* encapsulated in SA wall material during 60 days of storage at 4 °C. (SA-1: 130 °C, 10 mL/min; SA-2: 130 °C, 15 mL/min; SA-3: 160 °C, 10 mL/min; SA-4: 160 °C, 15 mL/min)

Table 1 The survival rates and encapsulation yield of *L. acidophilus* following the spray-drying process

Sample code	Inlet air temperature (°C)	Pump Rate (mL/min)	Outlet temperature (°C)	aw	Initial Microorganism Load (log cfu/g)	Survival counts after spray drying (log cfu/g)	Encapsulation yied (%)
SA-HPI-1	130	10	70	0.221 ± 0.001^{c}	8.76	7.86 ± 0.05^{ab}	12.85 ± 1.11^{a}
SA-1	130	10	68	0.229 ± 0.002^{ab}	8.74	7.42 ± 0.12^{cd}	4.78 ± 1.32^{d}
SA-HPI-2	130	15	65	0.234 ± 0.001^{a}	8.76	7.76 ± 0.01^{b}	10.00 ± 0.17^{ab}
SA-2	130	15	67	0.226 ± 0.003^{bc}	8.72	7.35 ± 0.09^{cde}	4.26 ± 0.88^{de}
SA-HPI-3	160	10	82	0.185 ± 0.004^{gh}	8.75	7.12 ± 0.04^{efg}	2.34 ± 0.19^{e}
SA-3	160	10	80	0.192 ± 0.001^{fg}	8.71	6.88 ± 0.15^{ghi}	1.47 ± 0.51^{fg}
SA-HPI-4	160	15	80	0.191 ± 0.001^{fg}	8.75	7.28 ± 0.02^{de}	3.38 ± 0.18^{de}
SA-4	160	15	78	0.198 ± 0.002^{ef}	8.74	6.95 ± 0.11^{fgh}	1.62 ± 0.41^{fg}
GA-HPI-1	130	10	60	0.214 ± 0.003^{d}	8.92	7.73 ± 0.17^{b}	6.46 ± 2.56^{bcd}
GA-1	130	10	63	0.208 ± 0.002^{d}	8.90	7.20 ± 0.08^{def}	1.99 ± 0.37^{fg}
GA-HPI-2	130	15	58	0.220 ± 0.001^{c}	8.92	7.85 ± 0.01^{ab}	8.51 ± 0.18^{bc}
GA-2	130	15	60	0.213 ± 0.001^{d}	8.91	7.15 ± 0.14^{defg}	1.73 ± 0.56^{fg}
GA-HPI-3	160	10	68	0.190 ± 0.001^{fg}	9.4	7.61 ± 0.09^{bc}	1.62 ± 1.01^{cde}
GA-3	160	10	71	0.182 ± 0.002^{h}	9.3	6.62 ± 0.05^{i}	0.20 ± 0.02^{h}
GA-HPI-4	160	15	65	0.200 ± 0.001^{e}	9.4	8.06 ± 0.08^{a}	4.57 ± 0.86^{d}
GA-4	160	15	69	0.188 ± 0.003^{g}	9.4	6.75 ± 0.10^{hi}	0.22 ± 0.05^{h}

SA-HPI Sodium alginate-hazelnut protein isolate conjugate, *SA* Sodium alginate control, *GA-HPI* Gum Arabic-hazelnut protein isolate conjugate, *GA* Gum Arabic control. *aw* Water activity of spray-dried powders. Encapsulation Yield (%), Calculated based on the microbial survival counts using the non-logarithmic viability ratio. $^{a-i}$ Different lowercase letters in the same column indicate statistically significant differences between samples according to Tukey's test ($P<0.05$)

As shown in Table 1, the inlet air temperature significantly affected both survival rates and encapsulation yield ($P<0.05$). For the SA-HPI matrix, increasing the temperature from 130 °C to 160 °C led to a decrease in survival counts from 7.86 to 7.12 log CFU/g at 10 mL/min pump rate. This reduction is attributed to the thermal denaturation of cellular proteins and damage to the cytoplasmic membrane of *L. acidophilus* at higher temperatures. Interestingly, the highest survival count (8.06±0.08 log CFU/g) was recorded in the GA-HPI-4 sample, suggesting that the gum arabic-protein conjugate might provide a more robust heat-shielding effect at specific flow rates. The conjugation of HPI with sodium alginate or gum Arabic significantly increased the Encapsulation Yield (EY %) compared with the control groups. The presence of HPI provided a superior protective matrix, preserving cell membrane integrity against thermal stress during atomization. The encapsulation yield (EY) varied significantly, ranging from 1.62% to 12.85%, across all samples. The highest yield was achieved using the SA-HPI matrix at the SA-HPI-1 sample. Generally, lower inlet temperatures favored higher yields, likely due to reduced particle stickiness and improved retention of the core material within the matrix. At 160 °C, a sharp decline in EY was observed for both wall materials, which may be attributed to rapid moisture evaporation, leading to premature crust formation or particle rupture and thereby reducing entrapment efficiency. Furthermore, the pump rate also influenced encapsulation efficiency. At a constant temperature of 130 °C, increasing the pump rate from 10 to 15 mL/min resulted in a slight decrease in yield for SA-HPI but an increase for GA-HPI; however, the difference was not significant ($P>0.05$). This suggests that the optimal feed rate is dependent on the rheological properties and film-forming capabilities of the specific wall material used. In conclusion, the combination of SA-HPI at 130 °C with a 10 mL/min pump rate (SA-HPI-1) proved to be the most effective parameter set for maximizing both *L. acidophilus* survival and the encapsulation process efficiency. This may be attributed to the excellent film-forming properties and lower oxygen permeability of the alginate-protein matrix, which provides a denser physical barrier against heat transfer.

In Vitro Digestion and Survival Ratios

The survival rates of *L. acidophilus* encapsulated within SA-HPI and GA-HPI matrices during sequential exposure to simulated oral, gastric, and intestinal conditions are summarized in Table 2. Protecting probiotic cells against the harsh acidic environment of the stomach (low pH and enzymatic activity) is a primary objective of microencapsulation. The free cells exhibited extreme sensitivity to gastric conditions, with their viability dropping drastically to 1.38±0.10 log CFU/g after SGF exposure. In sharp contrast, all encapsulated formulations provided significant protection ($P<0.05$), maintaining viability levels between 6.01 and 6.86 log CFU/g (for HPI-SA) and 6.81 and 7.55 log CFU/g (for HPI-GA) at the end of the gastric phase. This improvement confirms that both sodium alginate-hazelnut protein isolate (SA-HPI) and gum arabic-hazelnut protein isolate (GA-HPI) matrices

effectively shield the bacteria from the detrimental effects of low pH and pepsin activity. Among the formulations, the GA-HPI-1 sample demonstrated the highest gastric survival ratio (66.07 ± 0.73%), suggesting that the gum arabic-protein conjugate forms a dense protective barrier that limits the diffusion of hydrogen ions into the capsule core. The control group (GA-1) showed significantly lower survival (39.81 ± 0.55%), demonstrating that HPI conjugation is essential for creating an effective acid diffusion barrier. For the SA-HPI group, the gastric survival ratios were generally lower than the GA-HPI group, except for the SA-HPI-3 sample (44.67 ± 0.46%), indicating that the wall material composition and spray-drying parameters significantly influence the acid resistance of the microcapsules. In contrast, its corresponding control group (SA-3) reached a significantly lower survival of 18.62 ± 0.25%. During the subsequent intestinal phase (SIF), a further decline in probiotic viability was observed for all samples. Probiotic bacteria are highly sensitive to bile salts, which induce cellular disintegration by compromising their cell walls. However, the presence of a conjugate-based membrane serves as a semi-permeable barrier, effectively attenuating the diffusion of bile salts and mitigating their cytotoxic impact on the encapsulated cells [22]. The final counts remained substantially higher than those of the free cells. The SA-HPI-2 and SA-HPI-3 samples exhibited the highest post-intestinal viability (6.48 and 6.39 log CFU/g, respectively), with SA-HPI-3 achieving the highest intestinal survival ratio of 18.62 ± 0.27%. Control samples (SA and GA series), as they lacked the structural complexity required to repel bile salt penetration, showed lower ratios than conjugate samples ($P < 0.05$). The higher survival of alginate-based capsules in the intestinal phase can be attributed to the pH-responsive nature of sodium alginate. Alginate matrices tend to remain stable or slightly shrink in acidic SGF but undergo swelling and gradual disintegration in the neutral/alkaline environment of the SIF, allowing controlled release of the probiotics [32] while still providing protection against bile salts. Conversely, the GA-HPI formulations showed lower survival rates in the intestinal phase than in the gastric phase. This could be due to the faster dissolution of gum arabic in the intestinal fluid, which may have exposed the probiotic cells to bile salts more rapidly. Overall, these results indicate that while GA-HPI provides superior protection against gastric acidity, SA-HPI matrices may offer better sustained stability throughout the entire gastrointestinal transit, particularly in the intestinal environment. These results clearly indicate that Sodium Alginate-Hazelnut Protein Isolate (SA-HPI) conjugates are superior to Gum Arabic-based ones for the targeted gastrointestinal delivery of *L. acidophilus.*

Storage Stability and Survival Ratio

Maintaining probiotic viability during storage is a fundamental challenge for the development of functional food

Table 2 The survival rates of *L. acidophilus* encapsulated within SA-HPI, GA-HPI, SA and GA matrices during sequential exposure to simulated oral, gastric, and intestinal conditions

Sample code	Inlet Temp. (°C)	Pump Rate (mL/min)	Post-drying viability (log CFU/g)	Post-gastric viability (log CFU/g)	Gastric survival ratio (%)	Post-intestinal viability (log CFU/g)	Intestinal survival ratio (%)
Free Cell	-	-	Nd	1.38 ± 0.10^{g}	Nd	0.66 ± 0.20^{i}	Nd
SA-HPI-1	130	10	7.86 ± 0.05^{ab}	6.10 ± 0.10^{de}	1.74 ± 0.03^{m}	5.91 ± 0.22^{bc}	1.12 ± 0.02^{fg}
SA-1	130	10	7.42 ± 0.12^{cd}	5.85 ± 0.12^{ef}	2.69 ± 0.05^{l}	5.10 ± 0.15^{ef}	0.48 ± 0.01^{i}
SA-HPI-2	130	15	7.76 ± 0.01^{b}	6.86 ± 0.18^{b}	12.59 ± 0.13^{h}	6.48 ± 0.01^{a}	5.25 ± 0.09^{b}
SA-2	130	15	7.35 ± 0.09^{cde}	6.20 ± 0.10^{cd}	7.08 ± 0.11^{j}	5.80 ± 0.12^{bcd}	2.82 ± 0.05^{e}
SA-HPI-3	160	10	7.12 ± 0.04^{efg}	6.77 ± 0.01^{b}	44.67 ± 0.46^{b}	6.39 ± 0.09^{a}	18.62 ± 0.27^{a}
SA-3	160	10	6.88 ± 0.15^{ghi}	6.15 ± 0.08^{cde}	18.62 ± 0.25^{f}	5.50 ± 0.10^{cde}	4.17 ± 0.09d
SA-HPI-4	160	15	7.28 ± 0.02^{de}	6.01 ± 0.17^{de}	5.37 ± 0.02^{k}	5.96 ± 0.03^{b}	4.79 ± 0.03^{c}
SA-4	160	15	6.95 ± 0.11^{fgh}	5.60 ± 0.14^{f}	4.47 ± 0.08^{k}	4.95 ± 0.18^{fg}	1.00 ± 0.04^{fgh}
GA-HPI-1	130	10	7.73 ± 0.17^{b}	7.55 ± 0.01^{a}	66.07 ± 0.73^{a}	5.81 ± 0.12^{bcd}	1.20 ± 0.01^{f}
GA-1	130	10	7.20 ± 0.08^{def}	6.80 ± 0.10^{b}	39.81 ± 0.55^{c}	5.15 ± 0.20^{ef}	0.89 ± 0.02^{gh}
GA-HPI-2	130	15	7.85 ± 0.01^{ab}	7.06 ± 0.06^{b}	16.22 ± 0.11^{g}	5.85 ± 0.15^{bcd}	1.00 ± 0.06^{fgh}
GA-2	130	15	7.15 ± 0.14^{defg}	6.45 ± 0.12^{c}	19.95 ± 0.30^{e}	5.20 ± 0.11^{ef}	1.12 ± 0.04^{fg}
GA-HPI-3	160	10	7.61 ± 0.09^{bc}	6.81 ± 0.01^{b}	15.85 ± 0.16^{g}	4.80 ± 0.10^{fg}	0.15 ± 0.02^{j}
GA-3	160	10	6.62 ± 0.05^{i}	5.90 ± 0.09^{def}	19.05 ± 0.22^{ef}	4.20 ± 0.15^{h}	0.38 ± 0.01^{ij}
GA-HPI-4	160	15	8.06 ± 0.08^{a}	7.03 ± 0.03^{b}	9.33 ± 0.07^{i}	5.45 ± 0.05^{de}	0.25 ± 0.04^{ij}
GA-4	160	15	6.75 ± 0.10^{hi}	6.10 ± 0.11^{de}	22.38 ± 0.40^{d}	4.65 ± 0.09^{g}	0.79 ± 0.03^{h}

Free Cell, Non-encapsulated *L. acidophilus*. *SA-HPI* Sodium alginate-hazelnut protein isolate conjugate, *SA* Sodium alginate control, *GA-HPI* Gum Arabic-hazelnut protein isolate conjugate, *GA* Gum Arabic control. Survival Ratio (%), Calculated as the percentage of viable cells remaining after each digestion stage relative to the initial counts after spray drying. $^{a-m}$ Different lowercase letters in the same column indicate statistically significant differences between samples according to Tukey's test ($P < 0.05$). *Nd* Not determined

ingredients. The survival counts and storage survival ratios of *L. acidophilus* encapsulated in sodium alginate-hazelnut protein isolate (SA-HPI) and gum arabic-hazelnut protein isolate (GA-HPI) matrices over a 60-day storage period are detailed in Table 3. At the beginning of the storage period (day 0), the initial viability of the encapsulated probiotics ranged from 7.12 to 8.06 log CFU/g. After 60 days of storage, a gradual decline in microbial counts was observed across all formulations; however, all samples maintained viability above the critical threshold of 6.0 log CFU/g, whereas the control samples frequently dipped below this level. This indicates that both SA-HPI and GA-HPI matrices successfully formed a protective barrier, limiting the cells' exposure to oxygen and moisture, the primary factors that cause probiotic degradation during storage. The storage survival ratio (SSR) provided significant insights into the long-term stability of the capsules ($P<0.05$). Among all tested conditions, the SA-HPI-3 sample exhibited the highest stability, with an SSR of 38.02 ± 0.07%. Although SA-HPI-3 had a lower initial post-drying viability (7.12 log CFU/g), its superior performance during storage suggests that the higher inlet temperature may have facilitated the formation of a more robust, less porous, or more glassy matrix structure. Such a structure is known to restrict the mobility of molecules and reduce the metabolic activity of the encapsulated cells, thereby enhancing their longevity. In contrast, the GA-HPI formulations generally exhibited lower storage survival rates than the SA-HPI group. Specifically, the GA-HPI-4 sample exhibited the lowest SSR at 2.19 ± 0.01%. This difference is likely attributed to the inherent hygroscopic nature of gum arabic, which facilitates moisture absorption from the environment during storage. The subsequent increase in water activity (a_w) may promote matrix plasticization, increase molecular mobility and oxygen permeability, and accelerate the inactivation kinetics of *L. acidophilus.* Furthermore, the higher pump rate in the GA-HPI-4 sample might have led to a thinner wall structure, providing less protection against environmental stressors over time. For the sodium alginate-based capsules (SA-HPI-1, SA-HPI-2, and SA-HPI-4), the survival ratios remained relatively consistent, ranging from 10.23% to 12.02%. These results suggest that sodium alginate, when combined with hazelnut protein, creates a thermodynamically stable environment for *L. acidophilus*. The synergistic effect between the protein isolate and the polysaccharides likely contributes to the structural integrity of the microcapsules, as confirmed by the SEM observations. Overall, the study demonstrates that the SA-HPI-3 formulation provides the most effective long-term protection for *L. acidophilus*, making it a promising candidate for use in shelf-stable functional food applications. The decrease in *L. acidophilus* viability during storage is consistent with a first-order kinetic model. The regression equations presented in Figs. 1 and 2 quantitatively demonstrate the effects of different wall materials and process parameters on probiotic stability. GA-HPI conjugate matrix maintained viability quite well during the first 15 days, but a breakdown

Table 3 Stability of microencapsulated *Lactobacillus acidophilus* during 60 days of storage at 4 °C

Sample code	Inlet air temperature (°C)	Pump rate (mL/min)	Post-drying viability (log CFU/g)	Survival counts after 15-day storage (log cfu/g)	Survival counts after 30-day storage (log cfu/g)	Survival counts after 60-day storage (log cfu/g)	Storage survival ratio (%)
SA-HPI-1	130	10	7.86 ± 0.05^{ab}	7.27 ± 0.03^{bc}	6.97 ± 0.07^{cd}	6.87 ± 0.03^{a}	10.23 ± 0.03^{c}
SA-1	130	10	7.42 ± 0.12	6.85 ± 0.08^{de}	6.20 ± 0.11^{ef}	5.85 ± 0.09^{d}	$2.69+0.15^{g}$
SA-HPI-2	130	15	7.76 ± 0.01^{b}	6.98 ± 0.06^{cd}	6.79 ± 0.04^{d}	6.78 ± 0.06^{ab}	10.47 ± 0.07^{c}
SA-2	130	15	7.35 ± 0.09	6.70 ± 0.15^{def}	6.12 ± 0.07^{ef}	5.72 ± 0.14^{de}	$2.34+0.22^{gh}$
SA-HPI-3	160	10	7.12 ± 0.04^{c}	7.05 ± 0.14^{cd}	6.83 ± 0.09^{d}	6.70 ± 0.14^{abc}	38.02 ± 0.07^{a}
SA-3	160	10	6.88 ± 0.15	6.10 ± 0.06^{hij}	5.54 ± 0.12^{hi}	5.12 ± 0.08^{fgh}	$1.74+0.11^{ij}$
SA-HPI-4	160	15	7.28 ± 0.02^{c}	6.71 ± 0.12^{def}	6.40 ± 0.06^{e}	6.36 ± 0.12^{c}	12.02 ± 0.04^{b}
SA-4	160	15	6.95 ± 0.11	6.22 ± 0.09^{ghi}	5.68 ± 0.05^{gh}	5.25 ± 0.11^{fg}	$2.00+0.18^{hi}$
GA-HPI-1	130	10	7.73 ± 0.17^{b}	7.52 ± 0.27^{ab}	7.37 ± 0.23^{ab}	6.68 ± 0.27^{abc}	8.81 ± 0.02^{e}
GA-1	130	10	7.20 ± 0.08	6.55 ± 0.12^{efg}	5.95 ± 0.09^{fg}	5.42 ± 0.15^{ef}	$1.66+0.25^{ij}$
GA-HPI-2	130	15	7.85 ± 0.01^{ab}	7.73 ± 0.09^{a}	7.56 ± 0.11^{a}	6.70 ± 0.09^{abc}	7.08 ± 0.09^{f}
GA-2	130	15	7.15 ± 0.14	6.42 ± 0.07^{fgh}	5.80 ± 0.14^{gh}	5.30 ± 0.06^{fg}	$1.41+0.09^{j}$
GA-HPI-3	160	10	7.61 ± 0.09^{b}	7.51 ± 0.13^{ab}	7.44 ± 0.03^{ab}	6.59 ± 0.13^{abc}	9.44 ± 0.13^{d}
GA-3	160	10	6.62 ± 0.05	5.82 ± 0.11^{j}	5.20 ± 0.08^{j}	4.85 ± 0.12^{h}	$1.70+0.14^{ij}$
GA-HPI-4	160	15	8.06 ± 0.08^{a}	7.63 ± 0.18^{ab}	7.23 ± 0.06^{bc}	6.40 ± 0.18^{bc}	2.19 ± 0.01^{h}
GA-4	160	15	6.75 ± 0.10	5.95 ± 0.04^{ij}	5.35 ± 0.10^{ij}	4.92 ± 0.07^{gh}	$1.48+0.10^{j}$

A-HPI Sodium alginate-hazelnut protein isolate conjugate, *SA* Sodium alginate control, *GA-HPI* Gum Arabic-hazelnut protein isolate conjugate, *GA* Gum Arabic control. Storage Survival Ratio (%), Calculated as the ratio of the final microbial count (day 60) to the initial count after spray drying using non-logarithmic values. $^{a-j}$ Different lowercase letters in the same column indicate statistically significant differences between samples according to Tukey's test ($P<0.05$)

occurred after the 30th day of storage. Among the SA-HPI matrices, the SA-HPI-3 sample exhibited the lowest inactivation rates. This exceptional stability is attributed to strong electrostatic interactions and hydrogen bonding between the carboxyl groups of sodium alginate and the amino groups of hazelnut protein. The slope values in the control groups are approximately 2–4 times higher than those of the conjugates (Figs. 3 and 4). This indicates that pure wall materials are insufficient for protecting probiotics during storage compared to conjugated matrices. The synergistic interaction between the carboxyl groups of sodium alginate and the amino groups of hazelnut protein is suggested to create a dense barrier that may kinetically hinder the diffusion of oxygen and moisture, thereby reducing oxidative stress on *L. acidophilus*. Consequently, the oxidative stress and metabolic reactivation of *L. acidophilus* are kinetically hindered, as reflected in the low k values. Furthermore, the compact structure of SA-HPI at higher temperatures, as evidenced by the smoother SEM morphology, creates a tortuous path for environmental stressors, thereby extending the survivability of the encapsulated probiotics. Although the GA-HPI samples displayed gentle slopes in their kinetic plots, a faster loss of viability after the 15th day of storage. While gum arabic is an excellent film-former, its highly branched, complex heteropolysaccharide structure may yield a more porous matrix than the linear alginate chains when combined with hazelnut protein. The higher inactivation rates in the late storage period in GA-HPI could be linked to its higher hygroscopicity. Gum arabic tends to absorb more moisture from the environment during storage, potentially leading to plasticization of the matrix. In this rubbery state, the diffusion of oxygen and moisture increases exponentially, accelerating the degradation kinetics of the probiotic cells. The data suggest a synergistic effect between the inlet temperature and the type of polysaccharide. For SA-HPI, the higher temperature of 160 °C was beneficial for long-term kinetic stability, whereas for GA-HPI, lower temperatures of 130 °C seemed more favorable for maintaining a steady survival rate. These findings emphasize that the choice of wall material must be carefully balanced with spray-drying temperatures to optimize the shelf-life of functional probiotic ingredients.

Physical Properties and Microstructure Properties

The relationships among spray-drying parameters, water activity (aw), and the resulting microstructural morphology are critical for understanding the stability of encapsulated probiotics. The physical properties of the microcapsules and their corresponding SEM micrographs (Figs. 5 and 6) reveal distinct behaviors for both gum arabic-hazelnut protein (GA-HPI) and sodium alginate-hazelnut protein (SA-HPI) conjugates. The SEM analysis showed that GA-HPI microcapsules (Fig. 5A-D) were predominantly spherical with varying degrees of surface indentations. At a lower inlet temperature (130 °C), GA-HPI-1 (Fig. 5A) exhibited a more uniform and intact structure. The lower thermal stress during atomization facilitated controlled crust formation, preventing excessive expansion and resulting in a smoother surface. This structural integrity is consistent with the superior performance of GA-HPI-1 in gastric simulation tests. The observed surface smoothness and lack of visible fractures in GA-HPI-1 microcapsules indicate a robust physical barrier, which likely helps protect the core against simulated gastric fluid (SGF) by limiting acid diffusion. Conversely, as the inlet temperature increased to 160 °C (GA-HPI-3 and GA-HPI-4), surface concavities became more pronounced (Fig. 5C-D). Although GA-HPI-4 showed the highest post-drying viability (8.06 log CFU/g), its irregular surface topography may have facilitated oxygen diffusion through a potentially more porous or compromised matrix structure, leading to a lower storage survival ratio (SSR). In contrast, SA-HPI microcapsules (Fig. 6A-D) displayed a more rugose and shriveled appearance, a characteristic typical of the rapid drying kinetics and cross-linking nature of sodium alginate. The inclusion of hazelnut protein appeared to enhance the film-forming properties of the matrix, as no significant cracking, a common defect in pure alginate particles, was observed. SA-HPI-3 (Fig. 6C), produced at 160 °C, demonstrated a remarkably robust but shrunken morphology, indicating the formation of a dense matrix that effectively encapsulated the probiotic cells. Water activity (a_w) is a crucial factor in determining the shelf life of dried probiotics. As shown in the experimental data, increasing the inlet temperature from 130 °C to 160 °C resulted in a significant reduction in a_w for both systems. The SA-HPI system was more efficient at moisture removal, achieving higher outlet temperatures (up to 82 °C) and lower aw values (0.185–0.234) than the GA-HPI system (0.190–0.224). The exceptional storage stability of SA-HPI-3 (SSR = 38.02%) is directly linked to its ultra-low a_w (0.185 ± 0.004). The exceptionally low water activity observed in the SA-HPI-3 formulation suggests that the matrix is in a glassy state. This state potentially immobilizes the probiotic cells and restricts molecular mobility, which correlates with the significantly higher storage survival ratios observed. Furthermore, the impact of the pump rate was evident in the SA group, increasing the rate from 10 to 15 mL/min (SA-HPI-1 to SA-HPI-2) decreased the outlet temperature and increased a_w (0.221 to 0.234). This higher moisture content contributed to particle stickiness and the formation of the aggregates observed in the SEM clusters (Fig. 6A-B). Overall, the two wall materials offered different protective mechanisms. GA-HPI capsules were smoother and more spherical due

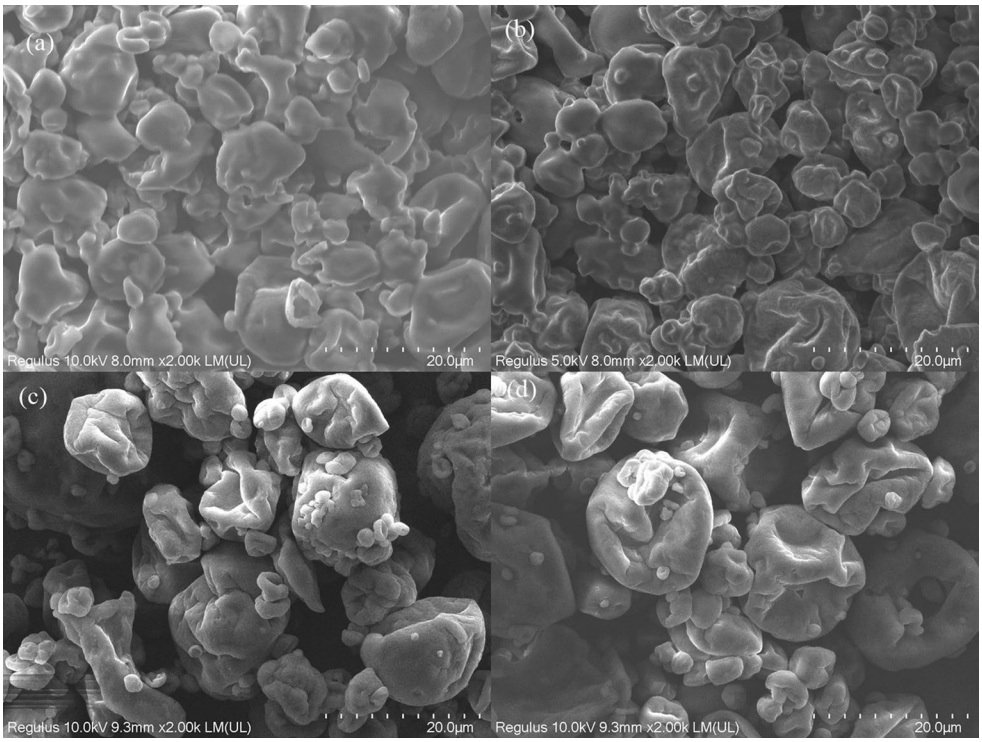


Fig. 5 Scanning electron micrographs (SEM) of GA-HPI conjugate microcapsules produced at different spray-drying conditions: (**A**) GA-HPI−1 (130 °C, 10 mL/min), (**B**) GA-HPI−2 (130 °C, 15 mL/min), (**C**) GA-HPI−3 (160 °C, 10 mL/min), (**D**) GA-HPI−4 (160 °C, 15 mL/min)

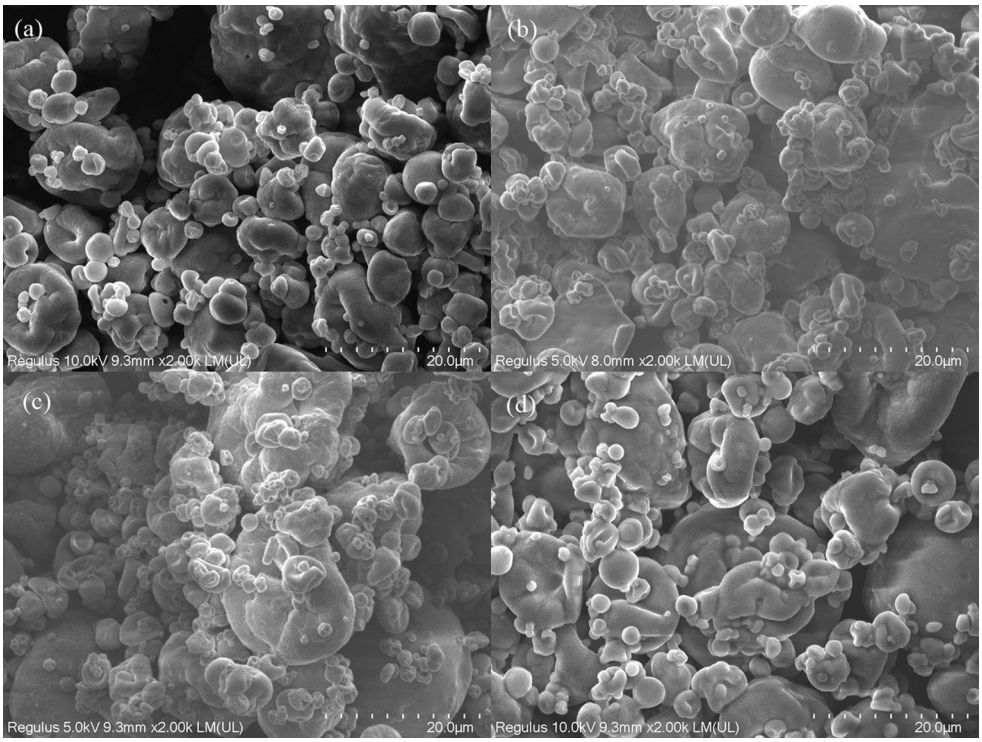


Fig. 6 Scanning electron micrographs of SA-HPI microcapsules produced at different spray-drying conditions: (**A**) SA-HPI−1 (130 °C, 10 mL/min), (**B**) SA-HPI−2 (130 °C, 15 mL/min), (**C**) SA-HPI−3 (160 °C, 10 mL/min), (**D**) SA-HPI−4 (160 °C, 15 mL/min)

to the superior emulsifying properties and lower viscosity of gum arabic, providing excellent initial protection and gastric resistance. On the other hand, the SA-HPI capsules, although more wrinkled, formed a denser, more rigid barrier. This rigid morphology, combined with lower a_w levels, proved more effective for long-term storage. Importantly, SEM images confirmed that for both matrices, *L. acidophilus* cells were successfully embedded within the core rather than being merely coated, as no free-standing bacteria or surface ruptures were observed in the optimized samples.

Conclusion

This study successfully demonstrated the potential of hazelnut protein isolate (HPI) conjugates with sodium alginate (SA) or gum arabic (GA) as novel wall materials for the spray-drying microencapsulation of *L. acidophilus*. The results revealed that processing parameters and the choice of polysaccharide significantly dictate the physical, morphological, and protective characteristics of the resulting microcapsules. All formulations maintained probiotic viability above the therapeutic threshold ($>10^6$ CFU/g) post-drying. The highest survival rate was observed in the GA-HPI-4 formulation, whereas the SA-HPI-1 sample yielded the highest encapsulation efficiency (12.8%). Encapsulation provided a robust shield against harsh gastric conditions compared to free cells. GA-HPI matrices showed superior performance in simulated gastric fluids, while SA-HPI matrices demonstrated better-sustained stability and potential for controlled release during the intestinal phase. A strong correlation was established between water activity (a_w), surface morphology, and long-term viability. The SA-HPI-3 formulation (160 °C inlet temperature, 10mL/min pump rate) emerged as the most stable candidate, achieving the lowest aw (0.185) and the highest storage survival ratio (38.02%) over 60 days. Compared to pure polysaccharide controls, HPI-conjugates provide a multi-layered defense mechanism. While pure SA and GA are susceptible to rapid degradation in gastric acid and provide limited protection during storage, the addition of hazelnut protein creates a synergistic shield that ensures higher microbial delivery to the lower intestine. This stability is attributed to the formation of a dense, glassy matrix as evidenced by SEM analysis. SEM observations confirmed that GA-HPI produced smoother, more spherical particles, while SA-HPI resulted in more wrinkled but structurally rigid capsules. Both systems successfully embedded probiotic cells without significant surface fractures. In conclusion, the synergistic use of hazelnut protein and polysaccharides offers a promising plant-based alternative for protecting sensitive probiotics. Specifically, the SA-HPI-3 formulation is recommended for industrial applications requiring long-term shelf stability. Future research could focus on incorporating these microcapsules into actual food matrices to evaluate their sensory impact and functional performance. While the current findings strongly suggest that the SA-HPI conjugate system provides a protective environment characterized by low molecular mobility, further characterization using Differential Scanning Calorimetry (DSC) and Dynamic Mechanical Thermal Analysis (DMTA) is required to definitively determine the glass transition temperature (Tg) and structural density of these novel wall materials. The absence of quantitative surface characterization (e.g., specific surface area, porosity, pore size distribution) prevents definitive attribution of storage stability differences to specific morphological features. Future work should integrate techniques such as BET analysis or X-ray microtomography to establish structure–function relationships.

This study demonstrates the promising potential of HPI-polysaccharide conjugates; it is important to acknowledge methodological limitations. Due to the low solubility of HPI and the consequent risk of nozzle clogging, microcapsules formulated with HPI alone were not produced as direct control samples. The comparison between the highly vulnerable free cells and the stable conjugate-encapsulated probiotics suggests that the interaction between HPI and polysaccharides is essential for creating a functional protective barrier capable of surviving both the spray-drying process and gastrointestinal transit. Future studies should aim to incorporate such control groups, possibly by employing alternative dispersion techniques or modified protein isolates with enhanced solubility, to precisely delineate the individual and combined protective effects of the hazelnut protein and the polysaccharides.

Acknowledgements This research was supported by TUBİTAK (Project No: 123O911).

Author Contributions İlyas Atalar: Writing – original draft, Investigation, Formal analysis, Supervision, Conceptualization. Hatice Elen : Formal analysis. Abdullah Kurt: Writing – review & editing, Investigation, Conceptualization. Nevzat Konar: Writing – original draft, Investigation, Supervision, Conceptualization.

Funding Open access funding provided by the Scientific and Technological Research Council of Türkiye (TÜBİTAK). This research was supported by TUBİTAK (Project No: 123O911).

Data Availability Data will be made available on request.

Declarations

Consent for Publication All the authors have agreed for publication of this manuscript.

Ethical Approval This study does not involve any human or animal trials.

Consent to Participate All coauthors have provided their consent to participate in the creation of this manuscript.

Publication Consent All authors have granted consent for the publication of this manuscript.

Competing Interests The authors declare no competing interests.

Open Access This article is licensed under a Creative Commons Attribution 4.0 International License, which permits use, sharing, adaptation, distribution and reproduction in any medium or format, as long as you give appropriate credit to the original author(s) and the source, provide a link to the Creative Commons licence, and indicate if changes were made. The images or other third party material in this article are included in the article's Creative Commons licence, unless

indicated otherwise in a credit line to the material. If material is not included in the article's Creative Commons licence and your intended use is not permitted by statutory regulation or exceeds the permitted use, you will need to obtain permission directly from the copyright holder. To view a copy of this licence, visit http://creativecommons.org/licenses/by/4.0/.

References

1. N.C. Santos, R.L.J. Almeida, S.S. Monteiro et al., Food Bioprod. Process. **150**, 207 (2025). https://doi.org/10.1016/j.fbp.2025.01.011
2. H. Yao, B. Liu, L. He et al., Food Chem. **413** (2023). https://doi.org/10.1016/j.foodchem.2023.135596
3. K. Vivek, S. Mishra, R.C. Pradhan et al., Appl. Food Res. **3**, 100248 (2023). https://doi.org/10.1016/j.afres.2022.100248
4. M. Hamdi, P. Mudgil, S. Al Hashmi et al., Food Res. Int. **219**, 116941 (2025). https://doi.org/10.1016/j.foodres.2025.116941
5. A. Can Karaca, N.H. Low, M.T. Nickerson, Trends Food Sci. Technol. **42**, 5 (2015). https://doi.org/10.1016/j.tifs.2014.11.002
6. I. Atalar, M. Dervisoglu, L.W.T.-F. Sci, Technol. **60**, 751 (2015). https://doi.org/10.1016/j.lwt.2014.10.023
7. G. Sompach, A. Rodklongtan, S. Nitisinprasert, P. Chitprasert, Food Res. Int. **159**, 111651 (2022). https://doi.org/10.1016/j.foodres.2022.111651
8. H. Song, R. Li, L. Yang et al., Food Hydrocoll. **154**, 110126 (2024). https://doi.org/10.1016/j.foodhyd.2024.110126
9. K. Sridhar, S. Bouhallab, T. Croguennec et al., Trends Food Sci. Technol. **127**, 49 (2022). https://doi.org/10.1016/j.tifs.2022.07.006
10. I. Atalar, T. Sari, H. Elen et al., Food Res. Int. **221**, 117508 (2025). https://doi.org/10.1016/j.foodres.2025.117508
11. O. Gül, L.B. Gül, M.E. Parlak et al., Food Hydrocoll. **168** (2025). https://doi.org/10.1016/j.foodhyd.2025.111549
12. O. Gul, F.T. Saricaoglu, I. Atalar et al., Foods 12, (2023) https://doi.org/10.3390/foods12091791
13. M. Nikbakht Nasrabadi, A. Sedaghat Doost, R. Mezzenga, Food Hydrocoll. **118**, 106789 (2021). https://doi.org/10.1016/j.foodhyd.2021.106789
14. M. Nooshkam, M. Varidi, D.K. Verma, Food Res. Int. **131**, 109003 (2020). https://doi.org/10.1016/j.foodres.2020.109003
15. B. Hiller, P.C. Lorenzen, Food Res. Int. **43**, 1155 (2010). https://doi.org/10.1016/j.foodres.2010.02.006
16. R. Hu, D. Dong, J. Hu, H. Liu, Food Hydrocoll. **138**, 108457 (2023). https://doi.org/10.1016/j.foodhyd.2023.108457
17. Q. Guo, J. Tang, S. Li et al., Int. J. Biol. Macromol. **216**, 124 (2022). https://doi.org/10.1016/j.ijbiomac.2022.06.207
18. R.R. Naik, Q. Ye, Y. Wang, C. Selomulya, Future Foods. **9**, 100380 (2024). https://doi.org/10.1016/j.fufo.2024.100380
19. B.C.S. Lima, L. de Carvalho, M.H. Nogueira et al., Int. J. Biol. Macromol. **316** (2025). https://doi.org/10.1016/j.ijbiomac.2025.144793
20. X. Kan, Z. Dai, D. Chen et al., Food Hydrocoll. **145**, 109137 (2023). https://doi.org/10.1016/j.foodhyd.2023.109137
21. Y. Yang, F. Niu, S.W. Cui et al., Food Hydrocoll. **132**, 107842 (2022). https://doi.org/10.1016/j.foodhyd.2022.107842
22. L. Mao, Q. Pan, Z. Hou et al., Food Hydrocoll. **84**, 489 (2018). https://doi.org/10.1016/j.foodhyd.2018.06.037
23. M. Siddiquy, M. Ghamry, H. Golshany et al., Prog Org. Coat. **188**, 108201 (2024). https://doi.org/10.1016/j.porgcoat.2023.108201
24. J. Yu, Y. Zhang, J. Yan et al., Innov. Food Sci. Emerg. Technol. **74**, 1 (2021). https://doi.org/10.1016/j.ifset.2021.102840
25. C. Ke, L. Li, Carbohydr. Polym. **302**, 120430 (2023). https://doi.org/10.1016/j.carbpol.2022.120430
26. F.T. Saricaoglu, O. Gul, A. Besir, I. Atalar, J. Food Eng. **233**, 98 (2018). https://doi.org/10.1016/j.jfoodeng.2018.04.003
27. I. Atalar, T. Sari, H. Elen, et al Int. J. Biol. Macromol. **364** (2026). https://doi.org/10.1016/j.foodhyd.2018.06.037
28. S. Amiri, R. Rezaei Mokarram, M. Sowti Khiabani et al., Int. J. Biol. Macromol. **123**, 752 (2019). https://doi.org/10.1016/j.ijbiomac.2018.11.084
29. D. Semyonov, O. Ramon, E. Shimoni, LWT-Food Sci. Technol. **44**, 1844 (2011). https://doi.org/10.1016/j.lwt.2011.03.021
30. A. Brodkorb, L. Egger, M. Alminger et al., Nat. Protoc. **14**, 991 (2019). https://doi.org/10.1038/s41596-018-0119-1
31. O. Gul, I. Atalar, L.B. Gul, Food Sci. Technol. Int. **25** (2019). https://doi.org/10.1177/1082013219853462
32. C. Colin, E. Akpo, A. Perrin et al., Molecules. **29**, 11 (2024). https://doi.org/10.3390/molecules29112515

Publisher's Note Springer Nature remains neutral with regard to jurisdictional claims in published maps and institutional affiliations.